DMD Fast Forward. Published on August 8, 2006 as doi:10.1124/dmd.106.010488

DMD #10488

Characterization of ebastine, hydroxyebastine, and carebastine metabolism by human liver microsomes and expressed cytochrome P450 enzymes: major roles for CYP2J2 and CYP3A

Kwang-Hyeon Liu, Mi-Gyung Kim, Dong-Jun Lee, Yune-Jung Yoon, Min-Jung Kim, Ji-Hong Shon, Chang Soo Choi, Young Kil Choi, Zeuresenay Desta, and Jae-Gook Shin

Department of Pharmacology and PharmacoGenomics Research Center, Inje University College of Medicine, Busan, Korea (K-H L, M-G K, D-J L, Y-J Y, M-J K, J-H S, J-G S); Department of Surgery, Busan Paik Hospital, Busan, Korea (C-S C, Y-K C), Frontier Inje Research for Science and Technology, Inje University, Busan, Korea (K-H L), and Division of Clinical Pharmacology, Departments of Medicine and Pharmacology, Indiana University School of Medicine, Indiana (Z.D.), USA

DMD Fast Forward. Published on August 8, 2006 as DOI: 10.1124/dmd.106.010488
This article has not been copyedited and formatted. The final version may differ from this version.

Running title: ebastine metabolism by CYP2J2 and CYP3A

Address correspondence to:

Dr. Jae-Gook Shin, Dept. of Pharmacology and PharmacoGenomics Research Center, # 633-165, Gaegum-Dong, Busanjin-Gu, Busan 614-735, South Korea. E-mail: phshinjg@inje.ac.kr

Number of Text Pages: 13

Number of Tables: 2

Number of Figures: 5

Number of References: 17

Number of Words

In the Abstract: 263

In the Introduction: 286

In the Discussion: 1142

Abbreviations:

HLM, human liver microsomes; P450: cytochrome P450; thio-TEPA: triethylenethiophophoramide

Abstract

Ebastine undergoes extensive metabolism to form desalkylebastine and hydroxyebastine. Hydroxyebastine is subsequently metabolized to carebastine. Although CYP3A4 and CYP2J2 have been implicated in ebastine *N*-dealkylation and hydroxylation, the enzyme catalyzing the subsequent metabolic steps (conversion of hydroxyebastine to desalkylebastine and carebastine) have not been identified. Therefore, we used human liver microsomes (HLM) and expressed P450s to characterize the metabolism of ebastine and those of its metabolites, hydroxyebastine and carebastine. In HLM, ebastine was metabolized to desalkyl-, hydroxy-, and car-ebastine; hydroxyebastine to desalkyl- and car-ebastine; and carebastine to desalkylebastine. Of the 11 cDNA-expressed P450s, CYP3A4 was the main enzyme catalyzing the *N*-dealkylation of ebastine, hydroxyebastine and carebastine to desalkylebastine [intrinsic clearance (Cl_{int}) = 0.44, 1.05, and 0.16 μl/min/pmol P450, respectively]. Ebastine and hydroxyebastine were also dealkylated to desalkylebastine to some extent by CYP3A5. Ebastine hydroxylation to hydroxyebastine is mainly mediated by CYP2J2 (0.45μl/min/pmol P450; 22.5- and 7.5-fold higher than that for CYP3A4 and CYP3A5, respectively), while CYP2J2 and CYP3A4 contributed to the formation of carebastine from hydroxyebastine. These findings were supported by chemical inhibition and kinetic analysis studies in human liver microsomes. The Cl_{int} of hydroxyebastine was much higher than that of ebastine and carebastine, and carebastine was metabolically more stable than ebastine and hydroxyebastine. In conclusion, our data for the first time suggest that both CYP2J2 and CYP3A play important roles in ebastine sequential metabolism: dealkylation of ebastine and its metabolites is mainly catalyzed by CYP3A4 while the hydroxylation reactions are preferentially catalyzed by

CYP2J2. The present data will be very useful to understand the pharmacokinetics and drug-interaction of ebastine in vivo.

Introduction

Ebastine, a potent and selective histamine H_1-receptor antagonist, belongs to a second generation of nonsedating antihistamine but with negligible anticholinergic and antiserotonergic properties(Llupia et al., 2003). Ebastine undergoes extensively sequential metabolism in the liver (Hashizume et al., 1998; Hashizume et al., 2001). The major primary metabolites identified in human are hydroxy- and desalkyl-ebastine, and hydroxyebastine is further metabolized to carebastine. In vitro studies indicate that the formation of desalkyl- and hydroxy-ebastine from ebastine, are catalyzed by CYP3A4 and CYP2J2, respectively (Hashizume et al., 2002). The specific hepatic cytochrome P450 (P450) enzymes involved in hydroxy- and car-ebastine metabolism have not been identified so far, despite some information which could be obtained from the previously published pharmacokinetics of ebastine. After oral administration to experimental animals and humans, ebastine is almost completely metabolized to the pharmacologically active principle, the carboxylated metabolite (carebastine), and other inactive metabolite (desalkylebastine) (Yamaguchi et al., 1994; Rohatagi et al., 2001). The C_{max} value of hydroxyebastine, major metabolite of ebastine in vitro, was approximately 50 fold lower than that of carebastine in vivo (Kang et al., 2004). A recent study by Chaikin et al (2005) has reported that, ketoconazole, a potent inhibitor of CYP3A4-mediated metabolism, decreases the clearance of ebastine, leading to an accumulation of the ebastine, with little effect on the pharmacokinetics of carebastine. Since, however, they did not measure the change of intermediate metabolite, hydroxyebastine, it is still open question which P450 isoforms may contribute to the formation of carebastine.

The objective of this study was to identify and kinetically characterize in vitro the P450 isoforms responsible for the metabolism of ebastine and its metabolites. The information from these studies will allow better understanding of the factors affecting ebastine pharmacokinetics and drug interaction.

Materials and Methods

Chemicals and Reagents. Ebastine, desalkylebastine, hydroxyebastine, and carebastine were kindly donated by Almirall Prodesfarma, SA (Barcelona, Spain). Astemizole, coumarin, diethyldithiocarbamate, furafylline, ketoconazole, quinidine, sulfaphenazole, terfenadine, thio-TEPA, β-nicotinamide adenine dinucleotide phosphate, EDTA, $MgCl_2$, glucose-6-phosphate, and glucose-6-phosphate dehydrogenase were purchased from Sigma-Aldrich (St. Louis, MO). Solvents were HPLC grade (Fisher Scientific CO., Pittsburgh, PA, USA) and the other chemicals were of the highest quality available. Pooled (H161) or single-donor (H003, H056, and HK34) human liver microsomes (HLM), and eleven different human recombinant P450 isoforms 1A2, 2A6, 2B6, 2C8, 2C9, 2C19, 2D6, 2E1, 2J2, 3A4, and 3A5 (Supersomes®) were purchased from BD Gentest (Woburn, MA, USA). Human P450s 2A6, 2B6, 2C8, 2C9, 2C19, 2E1, 2J2, 3A4, and 3A5 are co-expressed with human P450 reductase and cytochrome b5, however, P450s 1A2 and 2D6 are only co-expressed with human P450-reductase. The manufacturer supplied information regarding protein concentration and P450 isoform content.

Metabolism of Ebastine and Its Metabolites in Human Liver Microsomes or expressed P450s. The optimal conditions for microsomal incubation were determined in the linear range for the formation of metabolites of ebastine, hydroxyebastine, and carebastine. The rates of formation of metabolites were proportional to incubation times up to 60 min and protein concentrations up to 1.0 mg/ml at 30 min. In all experiments, ebastine, hydroxyebastine, and carebastine were dissolved, and serially diluted with methanol to the required concentrations; the solvent was subsequently removed by evaporation to dryness, under reduced pressure with an AES2010 SpeedVac (Savant Instruments Inc., Holbrook, NY).

The incubation mixtures, containing either 25 µl of microsomes (2.5 mg protein/ml of stock, prepared from three different human liver microsomal preparations) or 25 µl of cDNA-expressed P450 (diluted to 200 pmol/ml with phosphate buffer, pH 7.4) and various concentrations of ebastine, hydroxyebastine or carebastine (0 to 100 µM) was reconstituted in 100 µM phosphate buffer (pH 7.4) and prewarmed for 5 min at 37ºC. The reaction was initiated by adding the NADPH-regenerating system (1.3 mM β-nicotinamide adenine dinucleotide phosphate, 3.3 mM glucose-6-phosphate, 3.3 mM $MgCl_2$, and 1.0 U/ml glucose-6-phosphate dehydrogenase) and further incubated (final volume of 250 µl) for 30 min at 37ºC in a shaking water bath. The reaction was terminated by placing the incubation tubes on ice and by immediately adding 100 µl of acetonitrile. After adding the internal standard (terfenadine, 1 µM), the mixture was centrifuged at 1000*g* for 5 min at 4ºC and aliquots of the supernatant were injected into an LC/MS/MS system.

Chemical Inhibition Studies with Human Liver Microsomes. Pooled HLM (H161, it is pooled from 27 individual microsomes) and a P450-selective inhibitor were added to an incubation mixture similar to that described above. Ebastine, hydroxyebastine, and carebastine concentrations were 5 μM. The P450 isoform-selective inhibitors used were furafylline (10 μM) for CYP1A2, coumarin for CYP2A6 (100 μM), thio-TEPA for CYP2B6 (5 μM), sulfaphenazole for CYP2C9 (10 μM), *S*-benzylnirvanol for CYP2C19 (1 μM), quinidine for CYP2D6 (10 μM), diethyldithiocarbamate for CYP2E1 (10 μM), and ketoconazole for CYP3A (1 μM). Astemizole (50 μM), substrate of CYP2J2 and CYP3A4, were used as competitive inhibitor. Except for the addition of P450 isoform-selective inhibitors, all other incubation conditions were similar to those described previously by our group(Shin et al., 1999; Shin et al., 2002). After adding the internal standard and centrifugation as described above, aliquots of the supernatant were analyzed on an LC/MS/MS system.

Analytical Procedures. The concentrations of desalkyl-, hydroxy-, and car-ebastine were measured by the LC/MS/MS as described elsewhere(Kang et al., 2004). The system consisted of an API 3000 LC/MS/MS system (Applied Biosystems, Foster City, CA) equipped with an electrospray ionization interface used to generate positive ions $[M+H]^+$. The compounds were separated on a reversed-phase column (Luna C_{18}, 2.0 mm i.d. × 50 mm, 3 μm particle size; Phenomenex, Torrance, CA) with an isocratic mobile phase consisting of acetonitrile and water (40/60, v/v) containing 0.1% formic acid. The mobile phase was eluted using an HP 1100 series pump (Agilent, Wilmington, DE) at 0.2 ml/min.

The turboion spray interface was operated in the positive ion mode at 5500V

and 375 °C. The operating conditions were determined as follows: nebulizing gas flow, 1.04 l/min; auxiliary gas flow, 4.0 l/min; curtain gas flow, 1.44 l/min; orifice voltage, 40 V; ring voltage, 350 V; collision gas (nitrogen) pressure, 3.58×10^{-5} Torr. The mass transition used for quantitation of hydroxyebastine, carebastine, and terfenadine were *m/z* 486.7 → 167.1, 500.6 → 167.1, and 472.7 → 436.0, respectively (collision energy 40 eV): that for desalkylebastine was *m/z* 268.4 → 167.1 (collision energy 15 eV). The analytical data were processed by Analyst software (version 1.2, Applied Biosystems, Foster City, CA)

Data Analysis. Results are expressed as means ± S.D. of estimates obtained from three different liver microsome preparations in duplicate experiments. The apparent kinetic parameters of ebastine, hydroxyebastine, and carebastine metabolism were determined by fitting the unweighted kinetic data from HLM and expressed P450s to a one-enzyme Michaelis-Menten equation or a sigmoidal (Hill) equation model ($V = V_{max} \cdot [S]^n/(K_m{}^n + [S]^n)$), or substrate inhibition model ($V = V_{max} / (1 + K_m/[S] + [S]/K_{si})$). Calculated parameters were maximum rate of metabolite formation (V_{max}), Michaelis constant (K_m), intrinsic clearance ($Cl_{int} = V_{max}/K_m$), Hill coefficient (n), and substrate inhibition constant (K_{si}). The percentages of inhibition were calculated by the ratio of the rate of metabolite formation with and without the specific inhibitor. Calculations were performed using WinNonlin software (Pharsight, Mountain View, CA).

DMD Fast Forward. Published on August 8, 2006 as DOI: 10.1124/dmd.106.010488
This article has not been copyedited and formatted. The final version may differ from this version.

Results and Discussion

We present here a detailed characterization of the in vitro metabolism of ebastine and its metabolites using human liver P450 enzymes as summarized in Fig. 1. We have demonstrated that: 1) ebastine undergoes primary oxidative hydroxylation of the methyl groups of the *tert*-butyl moiety of ebastine to hydroxyebastine and dealkylation at the alicyclic bond attached to the piperidine nitrogen to form desalkylebastine, and secondary metabolism to carebastine; 2) the major routes of ebastine metabolism is mainly catalyzed by CYP2J2, CYP3A4, and CYP3A5; and 3) CYP2J2 exhibits atypical kinetics. These data should provide a scientific base upon which to build focused clinical studies that will help in understanding the pharmacokinetics and pharmacogenetic factors influencing ebastine therapeutic efficacy, drug interactions, and safety.

The formation of metabolites followed simple Michaelis-Menten kinetics with 0~100 μM ebastine, hydroxyebastine or carebastine, suggesting the involvement of a single enzyme or more than one enzyme with similar affinity (Fig. 2). A similar kinetic profile has been observed with ebastine hydroxylation in human intestinal microsomes(Hashizume et al., 2002) and CYP2J2-mediated terfenadine hydroxylation in recombinant CYP2J2(Parikh et al., 2003). The kinetic parameters are summarized in Table 1. The formation of carebastine from hydroxyebastine by rCYP2J2 exhibited substrate inhibition (Fig. 3), unlike the kinetic data obtained in HLM, which were characterized by a hyperbolic Michaelis-Menten equation (Fig. 2). Comparison of the goodness-of-fit values generated from these data indicates that a substrate inhibition enzyme kinetic model provided a better fit than did other models. The corresponding Eadie-Hofstee plot indicated a “hook” in the upper region of this plot (Fig. 3B, inset),

DMD Fast Forward. Published on August 8, 2006 as DOI: 10.1124/dmd.106.010488
This article has not been copyedited and formatted. The final version may differ from this version.

which is characteristic of substrate inhibition. The K_m, V_{max}, and K_{si} estimated from these data, respectively, were 0.75 μM, 9.86 pmol/min/pmol P450, and 5.55 μM (Table 2). Similar substrate inhibition profiles have been observed previously with CYP2B6-mediated 8,14-dihydroxyefavirenz formation(Ward et al., 2003) and CYP3A-mediated triazolam hydroxylation(Schrag and Wienkers, 2001), which are suggestive of multiple substrate-binding sites (or multiple regions within a single active site). To our knowledge, this is the first report of CYP2J2-mediated substrate inhibition. Although this observation may have no clinical relevance because the expected concentrations of the hydroxyebastine in human plasma after taking usual dosage of ebastine(Kang et al., 2004) are much lower than the substrate inhibition constants we obtained here, it may offer insight into the characteristics of the enzyme.

We provide evidence that ebastine hydroxylation is predominantly catalyzed by CYP2J2. First, formation rates of hydroxyebastine were potently inhibited (~ 70%) by astemizole, a substrate of CYP2J2 and CYP3A4, and slightly inhibited by ketoconazole, a potent CYP3A-selective inhibitor (Fig. 4A). Second, expressed human CYP2J2 metabolized ebastine to hydroxyebastine, whereas other P450 isoforms did not (Fig. 5A). We also noted that recombinant human CYP3A4 formed hydroxyebastine from ebastine, but the contributions of this isoform to ebastine metabolism appear minor: 1) the Cl_{int} for hydroxyebastine formation by CYP3A4 was 22.5-fold lower than that obtained in recombinant human CYP2J2 (Table 2). 2) a CYP3A-specific inhibitor (ketoconazole) slightly inhibited (~ 25%) the rates of formation of hydroxyebastine in HLM (Fig. 4A). These qualitative findings are consistent with the earlier work which had reported that CYP2J2 is the predominant ebastine hydroxylase in human intestinal microsomes(Hashizume et al., 2002).

The specific hepatic P450 enzymes involved in hydroxy- and car-ebastine metabolism have not been identified so far. Both ketoconazole (CYP3A inhibitor) and astemizole (substrate of CYP2J2 and CYP3A4)(Matsumoto et al., 2003) markedly inhibited (> 82%) car- and desalkyl-ebastine formation (Fig. 4B and 4C). Human recombinant CYP2J2 and CYP3A4 formed carebastine from hydroxyebastine (Fig. 5B). Similar to desalkylebastine formation from ebastine, desalkylebastine formation from hydroxy- and car-ebastine was mediated by CYP3A enzyme only (Fig. 5). These results suggest that desalkylebastine formation from hydroxy- and car-ebastine was clearly mediated by CYP3A, and hydroxyebastine was oxidized to carebastine by CYP2J2 and CYP3A4. It would be interesting to consider the enzymes responsible for metabolism of terfenadine alcohol, which possesses chemical structural similarities to hydroxyebastine. Terfenadine alcohol also has two similar major metabolic pathways of carboxylation and *N*-dealkylation. Unlike hydroxyebastine, carboxylation of terfenadine alcohol are reported to be catalyzed predominantly by CYP3A4(Ling et al., 1995). However, they didn't evaluate CYP2J2-mediated metabolism. Based on recent results(Parikh et al., 2003) that had reported that CYP2J2 is major enzyme involved in terfenadine (structural analogue of ebastine) hydroxylation, we can speculate that CYP2J2 as well as CYP3A4 may be involved in terfenadine acid formation from terfenadine alcohol.

After oral administration to humans, ebastine is almost completely metabolized to car- and desalkyl-ebastine(Kang et al., 2004; Lasseter et al., 2004). It is inconsistent with the in vitro findings which reported that ebastine is predominantly metabolised to hydroxy- and desalkyl-ebastine(Hashizume et al., 1998; Hashizume et al., 2001; Hashizume et al., 2002). To clarify this, we performed in vitro metabolism study of ebastine as well as its metabolites, hydroxy- and car-ebastine, using human liver

microsomes. The intrinsic clearance of hydroxyebastine was much higher than that of ebastine and carebastine (Table 1). The ratio of maximum dealkylation rate (V_{max}) of hydroxyebastine was also higher than that of ebastine and carebastine. In contrast to hydroxyebastine, carebastine showed low enzyme affinity and metabolic rate, thus, resulting in relatively low metabolic clearance. In expressed P450s, the formation of hydroxy- and desalkyl-ebastine from ebastine was catalysed predominantly by CYP2J2 and CYP3A4, respectively (Table 2). When hydroxyebastine was used as a substrate, we concluded that CYP2J2 and CYP3A4 isoforms were responsible for oxidation of hydroxyebastine, while CYP3A4 and CYP3A5 were responsible for desalkylebastine formation. Kinetic analysis indicated that the intrinsic clearance of hydroxyebastine was much higher than that of ebastine and carebastine (Table 1). These results provide evidence that once the hydroxyebastine is formed, it undergoes a rapid biotransformation to yield car- and desalkyl-ebastine. Carebastine appears to be relatively metabolically stable to ebastine and hydroxyebastine, supporting the in vivo findings that carebastine is major metabolite of ebastine. In addition, it is important to note, however, that CYP2J2 is also expressed in the extra-hepatic tissues such as heart, intestine, and kidney. Therefore, in vitro metabolism study using extra-hepatic tissues such as intestinal microsomes is necessary to determine the contribution of extra-hepatic tissues in the metabolism of ebastine and its metabolites.

The identification of CYP2J2 as the catalyst of hydroxylation of ebastine and hydroxyebastine (Fig. 1) may allow us utilize ebastine to probe this enzyme system. Despite the identification of a growing list of clinically important drugs(Hashizume et al., 2001; Matsumoto et al., 2003; Parikh et al., 2003) and endogeneous substances(Wu et al., 1996; Hashizume et al., 2002) as substrates of CYP2J2 in vitro, it remains difficult to determine or predict its clinical consequences because of the unavailability

DMD Fast Forward. Published on August 8, 2006 as DOI: 10.1124/dmd.106.010488
This article has not been copyedited and formatted. The final version may differ from this version.

of a specific and safe probe to measure the activity of the enzyme in vivo. Our data indicate that ebastine hydroxylation is a specific in vitro reaction marker of CYP2J2 and may have utility as a phenotyping tool to study the role of this enzyme in human drug metabolism.

References

Chaikin P, Gillen MS, Malik M, Pentikis H, Rhodes GR and Roberts DJ (2005) Co-administration of ketoconazole with H1-antagonists ebastine and loratadine in healthy subjects: pharmacokinetic and pharmacodynamic effects. *Br J Clin Pharmacol* **59:**346-354.

Hashizume T, Imaoka S, Mise M, Terauchi Y, Fujii T, Miyazaki H, Kamataki T and Funae Y (2002) Involvement of CYP2J2 and CYP4F12 in the metabolism of ebastine in human intestinal microsomes. *J Pharmacol Exp Ther* **300:**298-304.

Hashizume T, Mise M, Matsumoto S, Terauchi Y, Fujii T, Imaoka S, Funae Y, Kamataki T and Miyazaki H (2001) A novel cytochrome P450 enzyme responsible for the metabolism of ebastine in monkey small intestine. *Drug Metab Dispos* **29:**798-805.

Hashizume T, Mise M, Terauchi Y, O L, Fujii T, Miyazaki H and Inaba T (1998) N-Dealkylation and hydroxylation of ebastine by human liver cytochrome P450. *Drug Metab Dispos* **26:**566-571.

Kang W, Liu KH, Ryu JY and Shin JG (2004) Simultaneous determination of ebastine and its three metabolites in plasma using liquid chromatography-tandem mass spectrometry. *J Chromatogr B Analyt Technol Biomed Life Sci* **813:**75-80.

Lasseter KC, Dilzer SC, Vargas R, Waldman S and Noveck RJ (2004) Pharmacokinetics and safety of ebastine in patients with impaired hepatic function compared with healthy volunteers: a phase I open-label study. *Clin Pharmacokinet* **43:**121-129.

Ling KH, Leeson GA, Burmaster SD, Hook RH, Reith MK and Cheng LK (1995) Metabolism of terfenadine associated with CYP3A(4) activity in human hepatic microsomes. *Drug Metab Dispos* **23:**631-636.

Llupia J, Gras J and Llenas J (2003) Comparative antiallergic effects of second-generation H1-antihistamines ebastine, cetirizine and loratadine in preclinical models. *Arzneimittelforschung* **53:**93-97.

Matsumoto S, Hirama T, Kim HJ, Nagata K and Yamazoe Y (2003) In vitro inhibition of human small intestinal and liver microsomal astemizole O-demethylation: different contribution of CYP2J2 in the small intestine and liver. *Xenobiotica* **33:**615-623.

Parikh S, Gagne P, Miller V, Crespi C, Thummel K and Patten C (2003) CYP2J2 and CYP4F12 are active for the metabolism of non-sedating antihistamines: Terfenadine and astemizole. *Drug Metab Rev* **35:**190.

Rohatagi S, Gillen M, Aubeneau M, Jan C, Pandit B, Jensen BK and Rhodes G (2001) Effect of age and gender on the pharmacokinetics of ebastine after single and repeated dosing in healthy subjects. *Int J Clin Pharmacol Ther* **39:**126-134.

Schrag ML and Wienkers LC (2001) Triazolam substrate inhibition: evidence of competition for heme-bound reactive oxygen within the CYP3A4 active site. *Adv Exp Med Biol* **500:**347-350.

Shin JG, Park JY, Kim MJ, Shon JH, Yoon YR, Cha IJ, Lee SS, Oh SW, Kim SW and Flockhart DA (2002) Inhibitory effects of tricyclic antidepressants (TCAs) on human cytochrome P450 enzymes in vitro: mechanism of drug interaction between TCAs and phenytoin. *Drug Metab Dispos* **30:**1102-1107.

Shin JG, Soukhova N and Flockhart DA (1999) Effect of antipsychotic drugs on human liver cytochrome P-450 (CYP) isoforms in vitro: preferential inhibition of CYP2D6. *Drug Metab Dispos* **27:**1078-1084.

Ward BA, Gorski JC, Jones DR, Hall SD, Flockhart DA and Desta Z (2003) The cytochrome P450 2B6 (CYP2B6) is the main catalyst of efavirenz primary and secondary metabolism: implication for HIV/AIDS therapy and utility of efavirenz as a substrate marker of CYP2B6 catalytic activity. *J Pharmacol Exp Ther* **306:**287-300.

Wu S, Moomaw CR, Tomer KB, Falck JR and Zeldin DC (1996) Molecular cloning and expression of CYP2J2, a human cytochrome P450 arachidonic acid epoxygenase highly expressed in heart. *J Biol Chem* **271:**3460-3468.

Yamaguchi T, Hashizume T, Matsuda M, Sakashita M, Fujii T, Sekine Y, Nakashima M and Uematsu T (1994) Pharmacokinetics of the H1-receptor antagonist ebastine and its active metabolite carebastine in healthy subjects. *Arzneimittelforschung* **44:**59-64.

Footnotes

This work was supported by a grant from the Ministry of Science and Technology, Korea (National Research Laboratory Program) and the Korea Health 21 R & D Project, Ministry of Health & Welfare, R. O. K (03-PJ10-PG13-GD01-0002).

DMD Fast Forward. Published on August 8, 2006 as DOI: 10.1124/dmd.106.010488
This article has not been copyedited and formatted. The final version may differ from this version.

Legends for figures

Figure 1. Proposed metabolic pathway of ebastine in human liver microsomes.

Figure 2. Kinetics for the metabolite formation from (A) ebastine, (B) hydroxyebastine, and (C) carebastine in three human liver microsomes.

An increasing concentration of substrates (0 – 100 μM) was incubated with human liver microsomes and a NADPH-generating system at 37 °C for 30 min. The velocity (pmol/min/mg protein) versus substrate concentration was fit to a Michaelis-Menten equation (*see Data Analysis*). Each point represents the average obtained from three different human liver microsomes.

Figure 3. Kinetics for the metabolite formation from (A) ebastine and (B) hydroxyebastine in recombinant human CYP2J2.

An increasing concentration of substrates (0 – 100 μM) was incubated with recombinant human CYP2J2 and a NADPH-generating system at 37 °C for 30 min. The velocity (pmol/min/pmol P450) versus ebastine or hydroxyebastine concentration was fit to a Michaelis-Menten equation or substrate inhibition equation (*see Data Analysis*). The corresponding Eadie-Hofstee plot (velocity versus velocity/hydroxyebastine concentration) is shown in the inset. Each point represents the average ± SD of triplicate incubations.

Figure 4. Effects of P450 isoform-selective inhibitors on the metabolism of ebastine (A), hydroxyebastine (B), and carebastine (C) by human liver microsomes

Ebastine, hydroxyebastine or carebastine (5 μM) was incubated with pooled human liver microsomes in the presence of various inhibitors. Data are presented as mean ± SD of triplicate determinations. FF, furafylline (10 μM); COU, coumarin (100 μM); TEPA, thio-TEPA (5 μM); SFZ, sulfaphenazole (10 μM); BEN, *S*-benzylnirvanol (1 μM); QND, quinidine (10 μM); DEDC, diethyldithiocarbamate (10 μM); KCZ, ketoconazole (1 μM); ATZ, astemizole (50 μM).

Figure 5. Representative plots of the formation of each metabolite from (A) ebastine, (B) hydroxyebastine, and (C) carebastine by c-DNA expressed human P450 isoforms.

Human cDNA-expressed P450s 1A2, 2A6, 2B6, 2C8, 2C9, 2C19, 2D6, 2E1, 2J2, 3A4, and 3A5 were incubated with 5 μM ebastine, hydroxyebastine, or carebastine. Data shown are averages of triplicate experiments.

DMD Fast Forward. Published on August 8, 2006 as DOI: 10.1124/dmd.106.010488
This article has not been copyedited and formatted. The final version may differ from this version.

Table 1. Kinetic parameters for the metabolism of ebastine, hydroxyebastine, and carebastine in human liver microsomes.

The values are estimated from nonlinear least regression analysis using WinNonlin.

Kinetic parameters		V_{max} (pmol/min/mg protein)	K_m (μM)	V_{max}/K_m (μl/min/mg protein)
Ebastine	Dealkylation	108.2 ± 29.6	17.5 ±2.3	6.18 ± 1.16
	Hydroxylation	10.9 ± 3.0	5.1 ± 1.3	2.14 ± 0.48
Hydroxyebastine	Dealkylation	456.4 ± 69.1	13.7 ± 3.8	33.3 ± 9.0
	Carboxylation	340.2 ± 64.1	8.9 ± 0.9	38.2 ± 6.5
Carebastine	Dealkylation	94.1 ± 27.0	61 ± 6.1	1.54 ± 0.51

DMD Fast Forward. Published on August 8, 2006 as DOI: 10.1124/dmd.106.010488
This article has not been copyedited and formatted. The final version may differ from this version.

Table 2. Kinetic parameters for the metabolism of ebastine, hydroxyebastine, and carebastine in recombinant human P450s.

The values are estimated from nonlinear least regression analysis using WinNonlin.

Kinetic parameters			V_{max} (pmol/min/pmol P450)	K_m (μM)	V_{max}/K_m (μl/min/pmol P450)
CYP 3A4	Ebastine	Dealkylation	3.34	7.67	0.44
		Hydroxylation	0.12	6.86	0.02
	Hydroxyebastine	Dealkylation	7.99	7.63	1.05
		Carboxylation	1.10	3.48	0.32
	Carebastine	Dealkylation	0.60	3.85	0.16
CYP 3A5	Ebastine	Dealkylation	0.74	5.56	0.13
		Hydroxylation	0.14	2.33	0.06
	Hydroxyebastine	Dealkylation	3.09	21.9	0.14
		Carboxylation	0.79	13.6	0.06
CYP 2J2	Ebastine	Hydroxylation	8.20	18.3	0.45
	Hydroxyebastine	Carboxylation	9.86	0.75	-

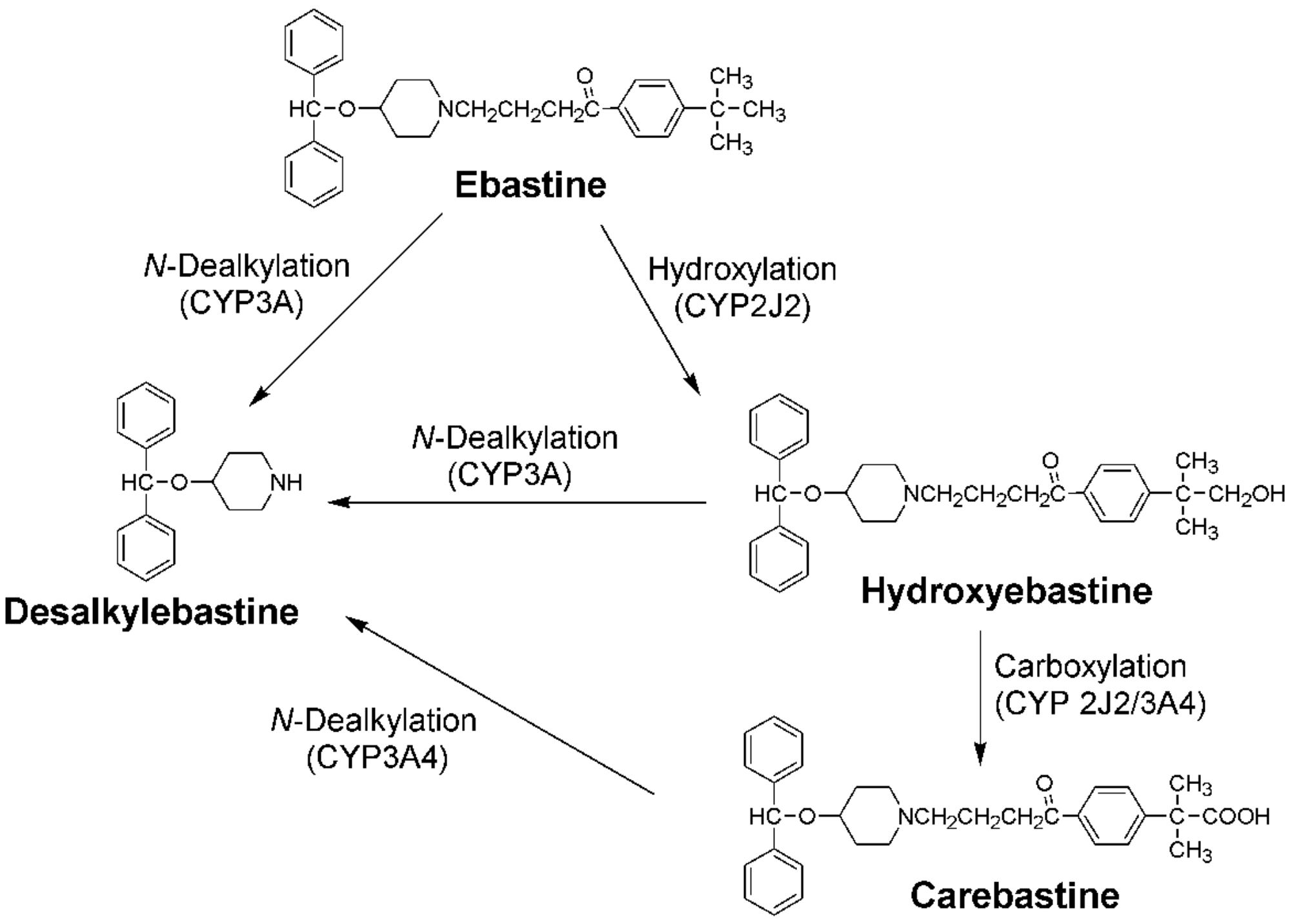
Ebastine
N-Dealkylation
(CYP3A)
Hydroxylation
(CYP2J2)
N-Dealkylation
(CYP3A)
Desalkylebastine
Hydroxyebastine
Carboxylation
(CYP 2J2/3A4)
N-Dealkylation
(CYP3A4)
Carebastine

Figure 1

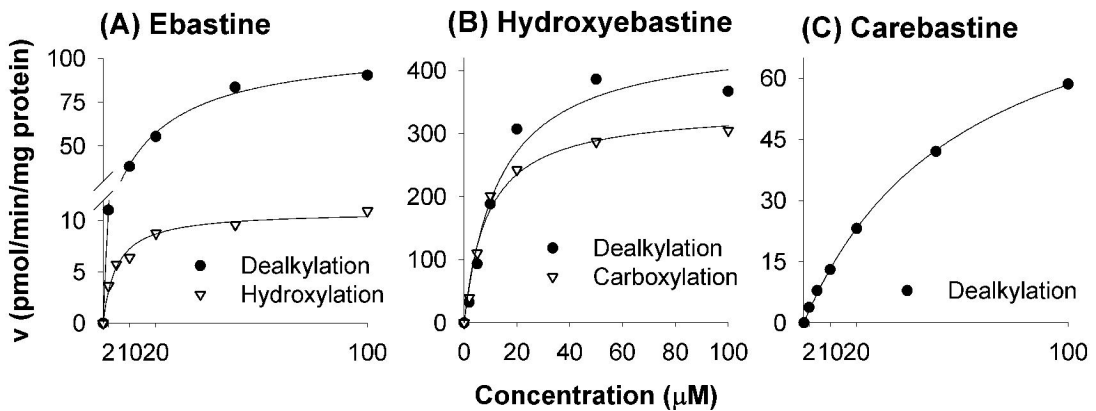
(A) Ebastine
(B) Hydroxyebastine
(C) Carebastine
v (pmol/min/mg protein)
Dealkylation
Hydroxylation
Dealkylation
Carboxylation
Dealkylation
Concentration (μM)

Figure 2

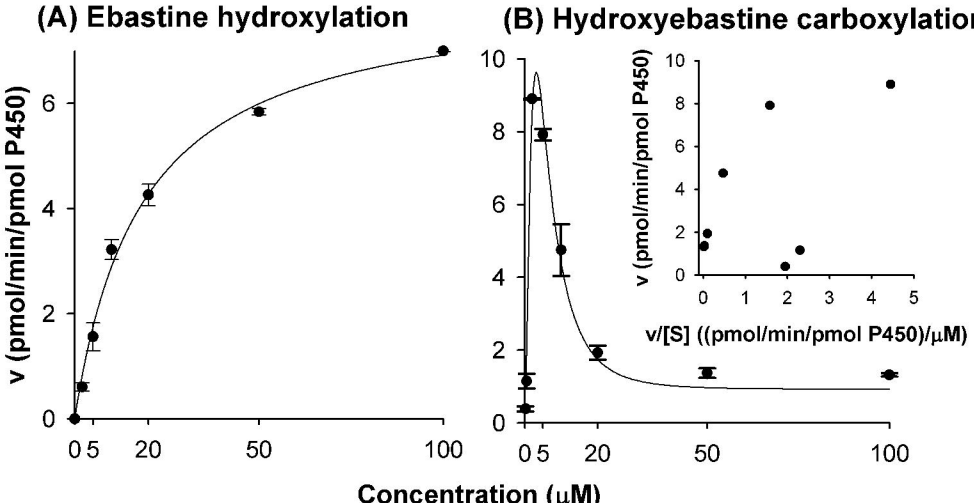
(A) Ebastine hydroxylation
(B) Hydroxyebastine carboxylation
v (pmol/min/pmol P450)
0
2
4
6
8
10
0 5
20
50
100
v (pmol/min/pmol P450)
0
1
2
3
4
5
v/[S] ((pmol/min/pmol P450)/μM)
Concentration (μM)

Figure 3

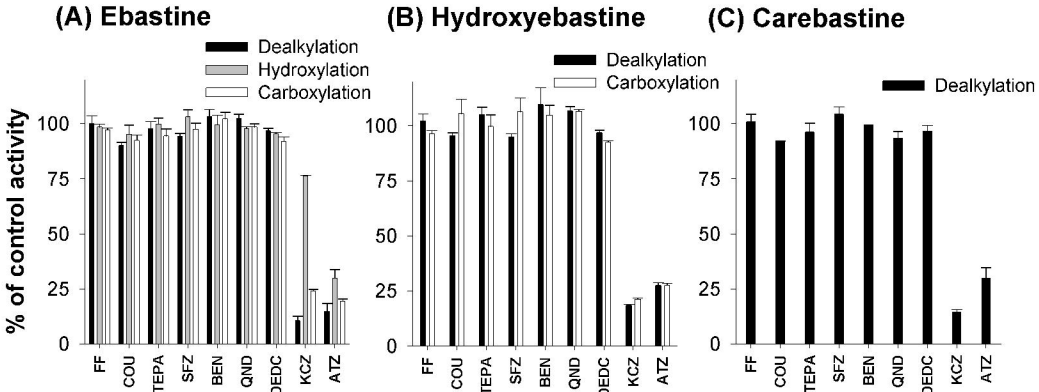
(A) Ebastine
Dealkylation
Hydroxylation
Carboxylation
% of control activity
100
75
50
25
0
FF
COU
TEPA
SFZ
BEN
QND
DEDC
KCZ
ATZ
(B) Hydroxyebastine
Dealkylation
Carboxylation
100
75
50
25
0
FF
COU
TEPA
SFZ
BEN
QND
DEDC
KCZ
ATZ
(C) Carebastine
Dealkylation
100
75
50
25
0
FF
COU
TEPA
SFZ
BEN
QND
DEDC
KCZ
ATZ

Figure 4

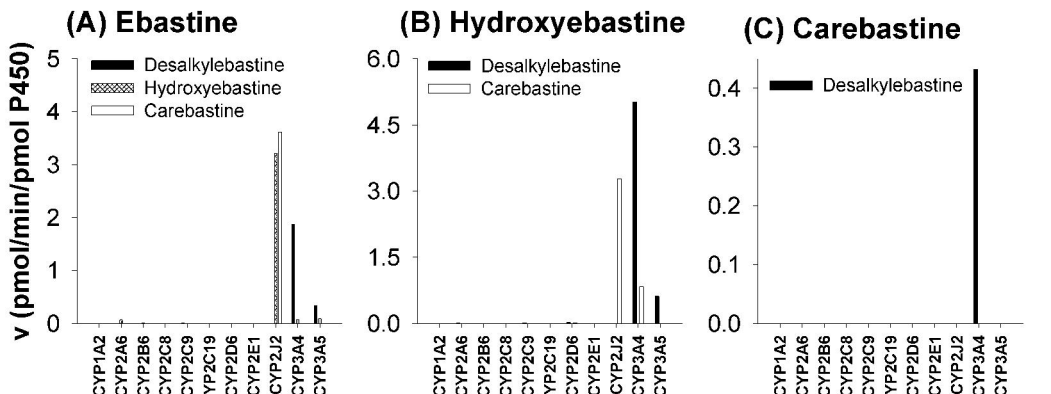
(A) Ebastine
(B) Hydroxyebastine
(C) Carebastine
v (pmol/min/pmol P450)
Desalkylebastine
Hydroxyebastine
Carebastine
CYP1A2
CYP2A6
CYP2B6
CYP2C8
CYP2C9
CYP2C19
CYP2D6
CYP2E1
CYP2J2
CYP3A4
CYP3A5

Figure 5